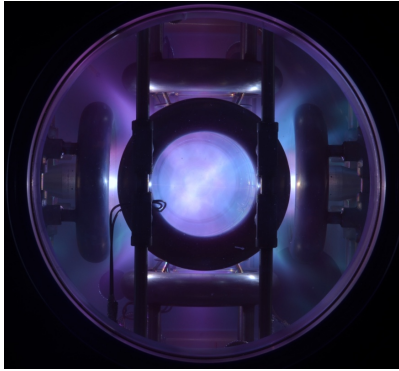


## Measurement of Enhanced Cusp Confinement at High Beta



Jaeyoung Park  
Energy Matter Conversion Corporation (EMC2)  
University of Maryland, September 9, 2014

1

## Fusion Research in 1958

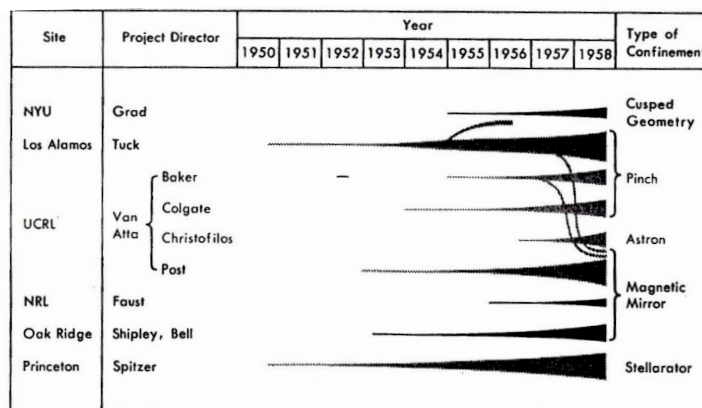
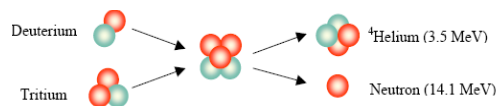
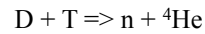


FIG. 19-2. CHRONOLOGY OF THE SHERWOOD PROGRAM, showing methods of plasma confinement in experiments to date.

From "Project Sherwood: The U. S. Program in Controlled Fusion" by Amasa Bishop (1958).

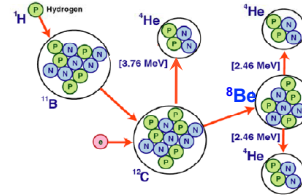
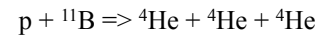
## Fusion Fuel Cycle Comparison

### D-T Fusion



- Most efficient fusion fuel
- Focus of existing DOE Program
- Significant production of radioactive materials

### p-<sup>11</sup>B Fusion



- Preferred fuel for fusion power
- No neutrons – minimal radiation
- Much more challenging than D-T due to high  $T_{\text{ion}}$  requirement and lower fusion output

EMC2 Proprietary

3

## Outline

- History of Magnetic Cusp Confinement
- Polywell Fusion:
  - Magnetic Cusp + Electric Fusion
- Recent Experiments at EMC2
- Future Work and Summary

4

## Motivation for Cusp Confinement

Reference: "Project Sherwood: The U. S. Program in Controlled Fusion" by Bishop (1958).

- Question on Plasma Stability by Teller in 1954

- "Attempts to contain a plasma as somewhat similar to contain jello using rubber bands"
- Basis of interchange instability (plasma version of Rayleigh Taylor instability) and idea of "good curvature" vs. "bad curvature"

- Preliminary analysis (by Frieman in 1955) indicated stellarator and magnetic mirror would be unstable not just at high  $\beta$  but at all values of  $\beta$ . ( $\beta = \text{plasma pressure/magnetic pressure}$ )

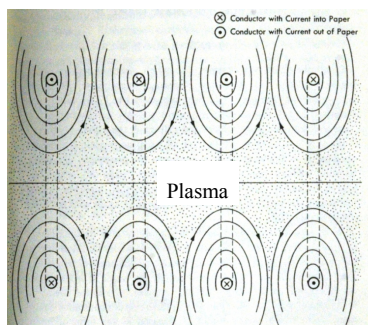
- By 1957, several concepts such as magnetic shear, field line tying and rotating plasmas were introduced to stabilize stellarator and mirror. However, it is understood that there would be undesirable limits on maximum plasma  $\beta$  in many of magnetic fusion concepts.

- ITER design calls for  $\beta$  to be 0.03, while the fusion power output scales as  $\beta^2$  for a fixed magnetic field value. H. York at Livermore was concerned that "the limitation on  $\beta$  might so reduce the net power output that this device (stellarator) could never be of economic interest" and started magnetic mirror program at Livermore.

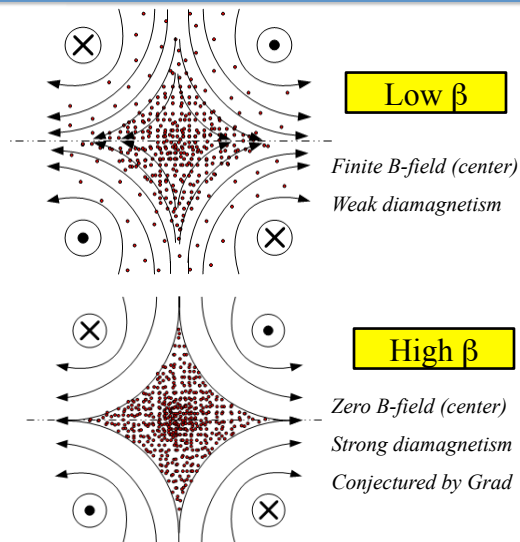
5

## Cusp Confinement Configuration

### Picket Fence

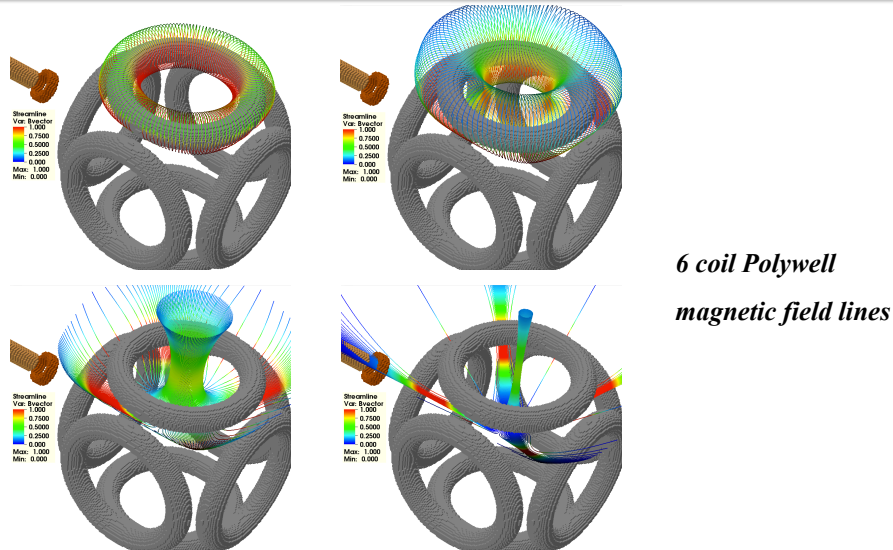


*Conceived by Tuck in 1954  
(from Bishop's book)*



6

## Polywell Cusp Magnetic Fields



7

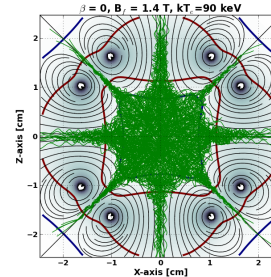
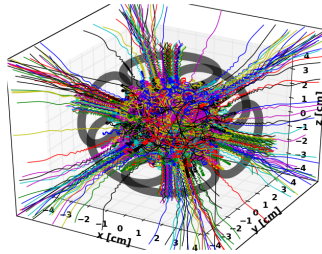
## Brief History of Cusp Confinement

- Picket-Fence (cusp confinement) concept by Tuck is the first stable magnetic confinement scheme against interchange instability. The entire region of confined plasma faces magnetic fields with good curvature. As such, good plasma stability has been observed in many cusp experiments.
- However, original picket fence approach was quickly abandoned due to rapid plasma loss along the open field lines, meaning good stability comes with bad confinement.
- Between 1955-1958, NYU group led by Grad investigated the case of high  $\beta$  confinement in magnetic cusp. **Their result was the plasma confinement would be greatly enhanced for a high  $\beta$  plasma in the cusp, compared to a low  $\beta$  plasma.**
- This confinement enhancement conjecture made the cusp approach to be promising. For the next 20 years, detailed experiments were conducted on ~20 different devices and ~200 papers were published related to the cusp confinement as a result. Two excellent review articles by Spalding (1971) and Haines (1977).
- However, most efforts on cusp confinement stopped by 1980 due to a lack of progress.

8



## Plasma Confinement in Cusp at Low $\beta$



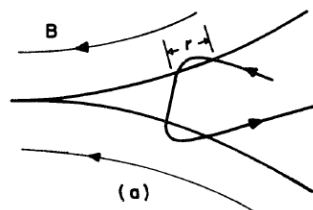
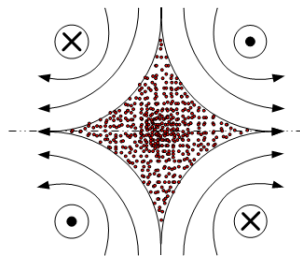
**Low  $\beta$  cusp** confinement can be modeled as “magnetic mirror” with particle transit time as a scattering time to loss cone: due to non-conserved magnetic moment near  $r=0$

$\tau_e(r_{coil}, E_e, B_{max}) \approx (2r_{coil} / v_e) \times M^*$  or  $\propto (r_{coil})^{1.75} \times E_e^{-7/8} \times B_{max}^{3/4}$   
 where  $v_e$  is a electron velocity at  $E_e$ ,  $M^*$  is an effective mirror ratio,  $B_{max}/B_{min}^*$   
 and  $B_{min}^*$  is given as  $\frac{1}{B} \times \frac{dB}{dr} (r = r_{adibatic}) = \frac{1}{A \times r_{Lamor}(E_e, B_{min}^* (r = r_{adibatic}))}$   
 and  $A$  is a constant between 3-5 for a given magnetic field profile

1  $\mu$ s confinement time  
 for 100 keV electron with 7  
 T, 1 m, 6 coil cusp – will not  
 work for a net power device

9

## Plasma Confinement in Cusp at High $\beta$



Berkowitz et al  
 1958 paper  
 “Cusped geometries”

In high  $\beta$  cusp, a **sharp transition layer exists between plasma and B-fields**. Plasma particles will undergo specular reflection at the boundary except for the particle moving almost exactly in the direction of the cusp. The loss rate will have gyro-radius scaling.

Theoretically conjectured

Loss current per cusp by Grad and NYU team

$$\frac{I_{e,i}}{e} = \frac{\pi}{9} n_{e,i} v_{e,i} \times \pi (r_{e,i}^{gyro})^2$$

0.5s confinement time  
 for 100 keV electron with 7 T, 1m,  
 6 coil cusp  $\rightarrow$  favorable for a net  
 power device.

10

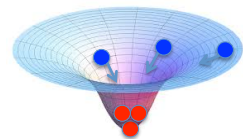
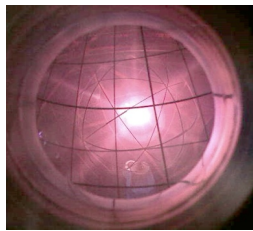
## What were the challenges on High $\beta$ cusp?

1. **How to form high  $\beta$  plasma in a leaky cusp: start up problem**
  - Use of (pulsed) high power plasma injectors or laser ablation
  - Typical injector produce cold plasmas 10-50 eV
  - $\beta=1$  plasma were achieved with strong diamagnetism and good stability
2. **Which loss rate is correct?**
  - Question on ion gyro-radius vs. electron gyro-radius
  - Ion gyro-radius will not work for fusion: experiments indicated ion gyro-radius
3. **How to heat initial cold plasmas to fusion relevant temperatures?**
  - Magnetic compression and shock heating was suggested and tried without much success.
4. **How to measure plasma confinement or confinement enhancement?**
  - Experiments lasted only for a short period (due to high power injector), while the predicted confinement time was long.

*Success on #1, but results on #2 appeared not favorable  
No promising solutions were presented for #3 and #4. → end of cusp by 1980*

11

## Electric Fusion



Deep negative potential well (1) accelerates and traps positive ions (2) until they generate fusion reactions

*Contributions from Farnsworth, Hirsch, Elmore, Tuck, Watson and others*

### Operating principles

(virtual cathode type )

- e-beam (or grid) accelerates electrons into center
- Injected electrons form potential well
- Potential well accelerates/confines ions
- Energetic ions generate fusion near the center

### Attributes

- **Excels in generating energetic ions with good confinement**
- But loss of high energy electrons is too large

**Net power generation is unlikely  
(present efficiency:  $1-10 \times 10^{-6}$ )**

12

## Polywell Fusion Principle

Combines two good ideas in fusion research: Bussard (1985)

**a) High  $\beta$  magnetic cusp:** High energy electron confinement in high  $\beta$  cusp: Bussard termed this as “wiffle-ball” (WB).

**b) Electric fusion:** High energy electron beams form a potential well, which accelerates and confines ions

Electric fusion provides

- Ion heating
- Ion confinement

for high  $\beta$  cusp

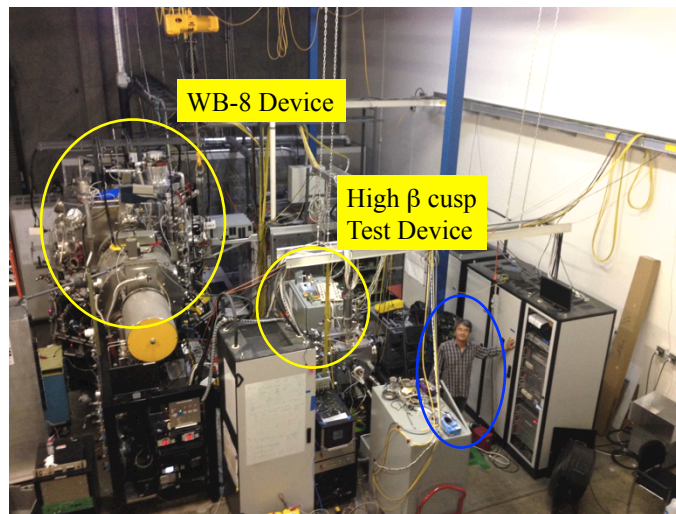
High  $\beta$  cusp provides

- High energy electron confinement

for electric fusion

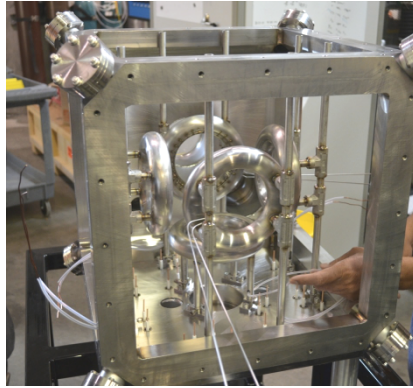
13

## Recent Experiments at EMC2 (EMC2 San Diego Facility)

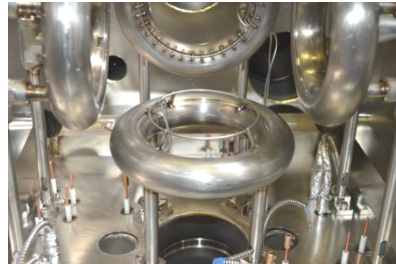


14

## High $\beta$ cusp test device installation



6 coil cusp installation



Locations of flux loop

15

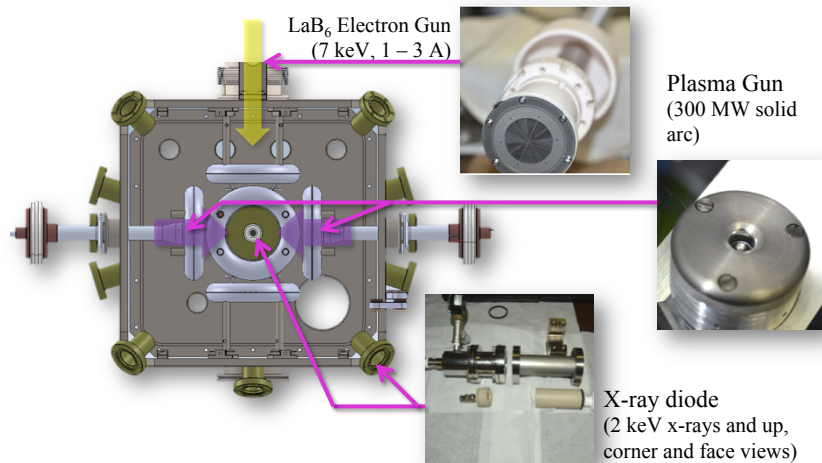
## Experimental Plan

1. Plasma injection to the cusp
  - Use high power arc (solid target) plasma injectors
2. Verify high  $\beta$  plasma formation in the cusp
  - Measurements on plasma density, magnetic flux and electron temperature
3. High energy electron injection to high  $\beta$  cusp
  - LaB<sub>6</sub> based electron beam injector, sufficient for diagnostics but not for potential well formation
4. Confinement measurement of high energy electrons in the cusp
  - Time resolved hard x-ray intensity from bremsstrahlung

Bulk (cold & dense) plasma from arc injectors provides plasma pressure (high  $\beta$ ) to modify cusp B-fields, while the confinement property is measured for high energy electrons in the cusp.

16

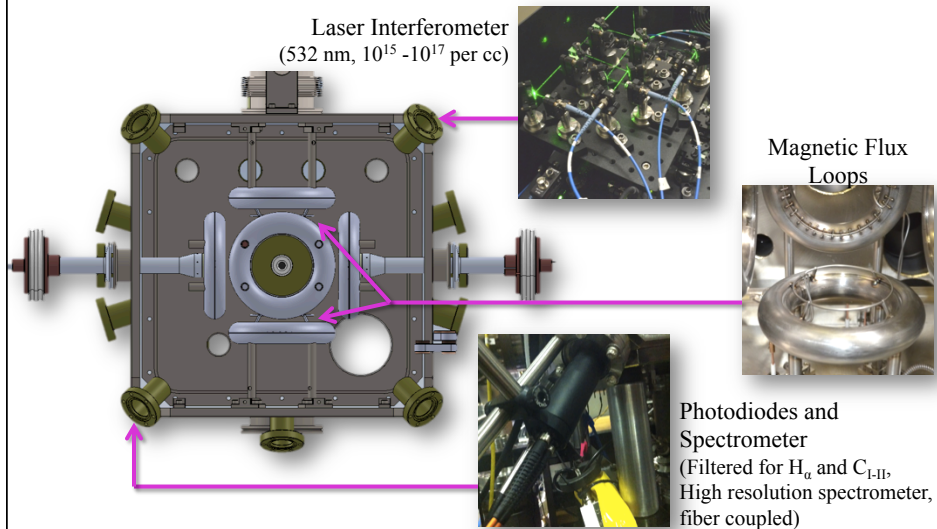
## Experimental Setup for high $\beta$ cusp confinement



Chamber size: 45 cm cube, Coil major radius; 6.9 cm  
Distance between two coils: 21.6 cm, B-field at cusp (near coil center) 0.6 – 2.7 kG

17

## Experimental Setup (continued)



18

## Solid arc plasma injector

Plasma injection by co-axial guns (j x B) using solid fuel

- Ignitron based pulse power system (40  $\mu$ F cap holds 3 kJ at 12kV)
- $\sim 100$  kA arc current  $\rightarrow \sim 300$  MW peak power and  $\sim 7$   $\mu$ s pulse
- $\beta=1$  @ 2.5 kG:  $1.5 \times 10^{16} \text{ cm}^{-3}$  at 10 eV or 100J in a 10 cm radius sphere



solid arc using  
polypropylene film  
2 mm A-K gap



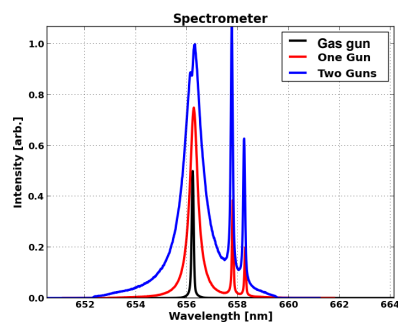
Animation of plasma injection



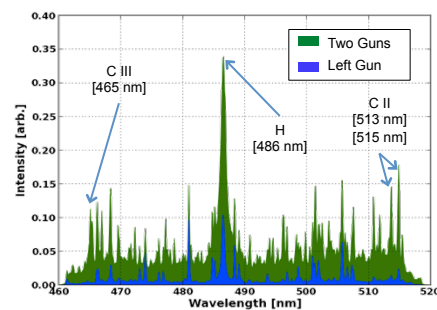
Dual arc plasma injection movie

19

## High $\beta$ plasma formation



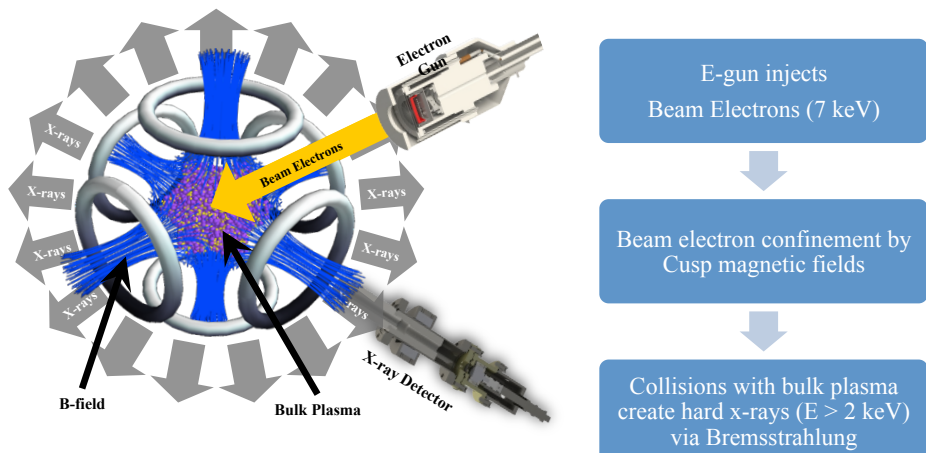
- Plasma density on the order of  $10^{16} \text{ cm}^{-3}$  from Stark broadening of  $H\alpha$  line
- Laser interferometer provides single shot line integrated density variation in time



- Electron temperature is estimated  $\sim 10$  eV from C II and CIII emission
- $H\alpha$ , C II line by photodiode and visible spectra by gated CCD is used to monitor  $T_e$  variation in time

20

## High energy electron beam produces hard x-rays



Transit time:  $\sim 7$  ns for 7 keV electron for 22 cm transit

Expected confinement time:  $\sim 45$  ns for low  $\beta$  and  $\sim 18$   $\mu$ s for high  $\beta$  (x400 increase)

21

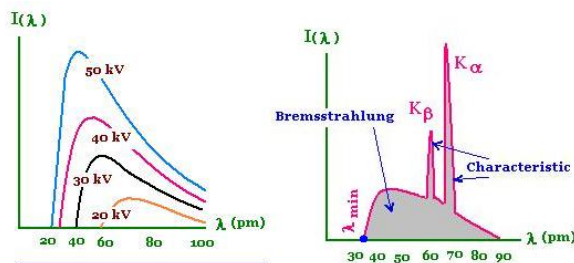
## Bremsstrahlung x-ray emission from interaction between beam electrons and plasma

Bremsstrahlung radiation from e-beam interaction with plasma ions

$$e + \text{ion} \rightarrow e + \text{ion} + h\nu \quad \longrightarrow \quad P^{Br} \propto n_e^{beam} E_{beam}^{1/2} n_{ion} Z_{eff}^2$$

### Bremsstrahlung x-ray intensity

→ Direct measurement of beam e-density inside Cusp

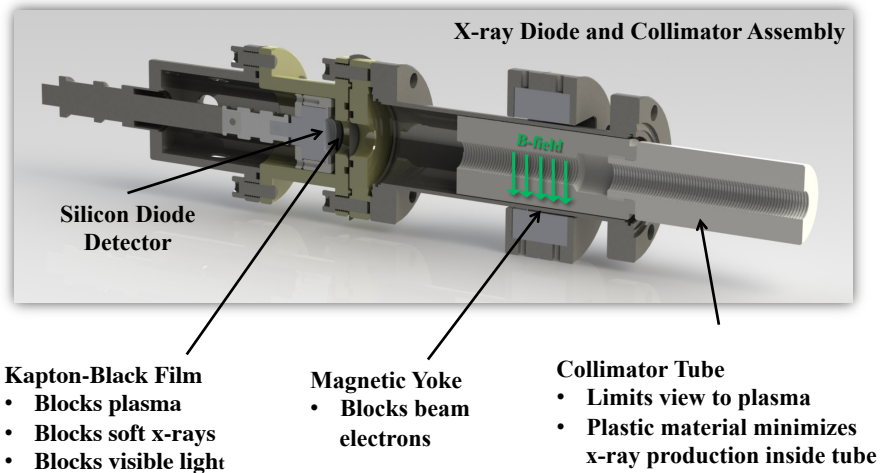


Careful measurement is required to eliminate spurious radiation from impurities, vacuum wall, coil surfaces, and characteristic line emission

22

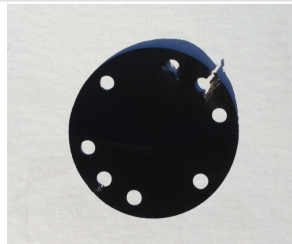


## X-ray collecting optics to eliminate unwanted signals

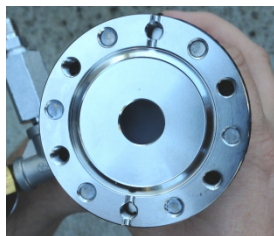


23

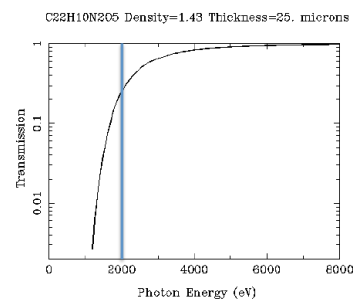
## Hard x-ray filter



25  $\mu\text{m}$  thick light tight Kapton filter  
(works as vacuum interface)



**Filter Transmission**



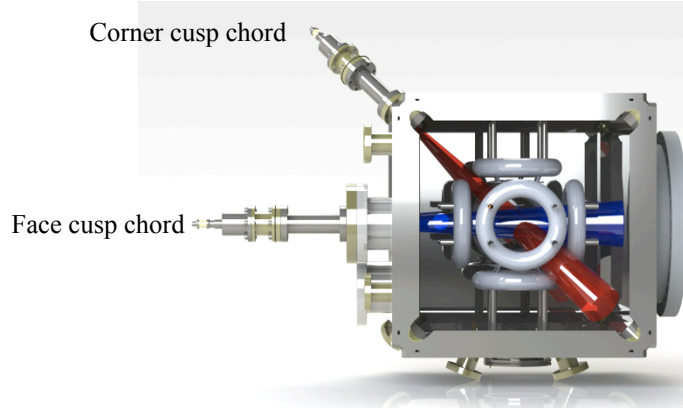
Filter has sharp cutoff at  $\sim 2$  keV photon energy

- blocks any characteristic x-ray emission from light elements up to  $^{14}\text{Si}$  and  $^{15}\text{P}$
- blocks UV-visible light from plasmas
- blocks charged particles from reaching the detector

24



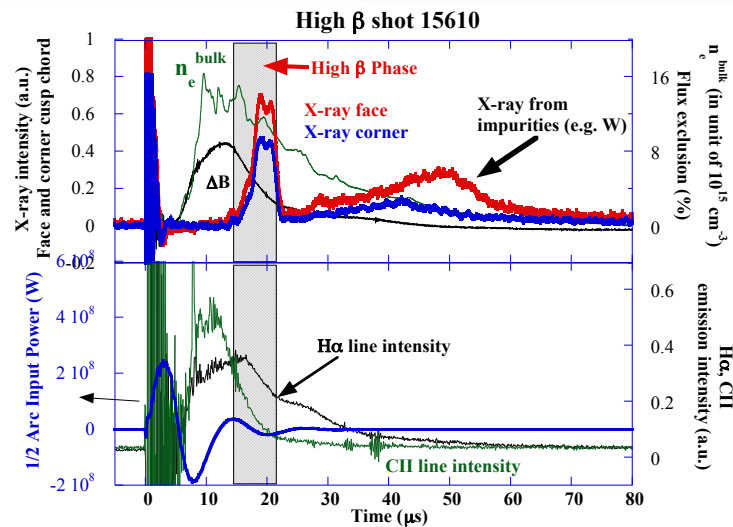
## Spatial collimation of x-ray detectors



- Collimation is designed to eliminate direct line-of-sight view of metal surfaces
- In addition, opposite sides of the chamber wall are covered using Kapton film and quartz window
- Both chords allow good volume averaging of x-ray emission from core plasmas

25

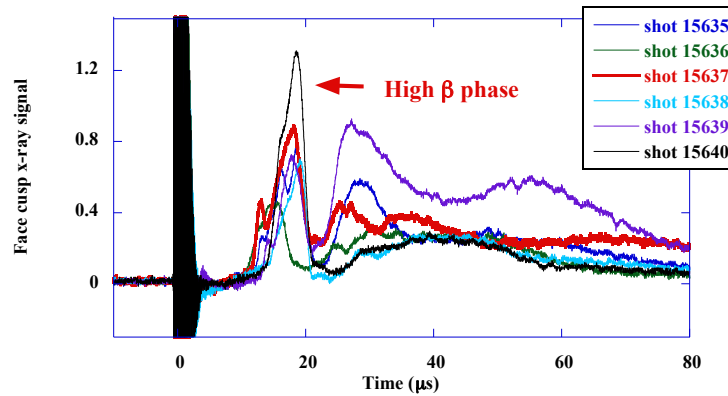
## First ever confirmation of high $\beta$ cusp confinement enhancement (October 23, 2013)



26

## Reproducibility of high $\beta$ cusp confinement

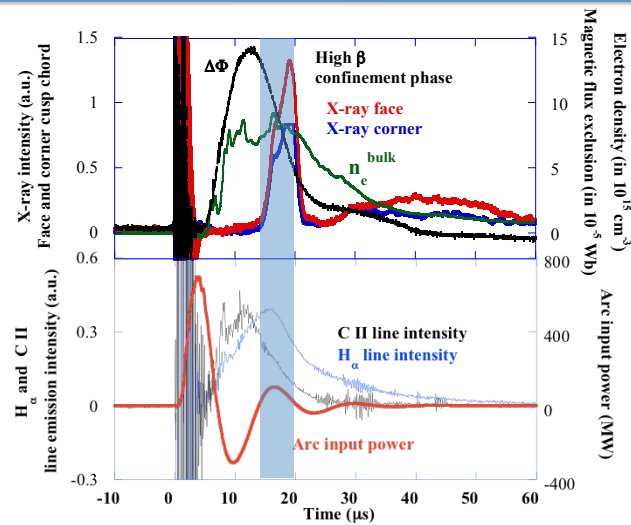
6 consecutive shots with  $\sim 200$  J of injected plasma energy at 2.7 kG B-fields  
 $\rightarrow$  estimated beta  $\sim 0.7$  and 10% measured flux exclusion



All six shots show distinctive high  $\beta$  phase  $\rightarrow$  good reproducibility

27

## High $\beta$ cusp shot 15640 (Oct 25, 2013)



- Hard x-ray signals exhibit very distinctive features between 14  $\mu$ s and 19  $\mu$ s

28

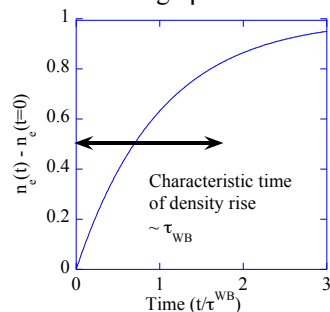
## How to interpret x-ray signals

- We have a set of data which shows that the broad x-ray peaks between 40-50  $\mu\text{s}$  come from e-beam interaction with Tungsten impurities.
- Electron beam turns on 30  $\mu\text{s}$  before plasma injection and turns off at  $t=150 \mu\text{s}$
- X-ray intensity is low (nearly zero) initially even after bulk density reaches its peak following plasma injection.
- Onset of the x-ray signal increases comes shortly after the peak of flux exclusion
- During the high  $\beta$  phase, the hard x-ray intensity from beam electron interaction with bulk plasma increases by a factor of  $\sim 20$  or more, while the bulk plasma density varies less than a factor of 2.
- At the end of the high  $\beta$  phase, the x-ray signals decrease very rapidly within 1-2  $\mu\text{s}$ . No other plasma quantities change this fast during this period. Since the x-ray measurement is volume averaged, the only possible explanation is a sudden decrease of beam electron confinement.
- Decay of high  $\beta$  phase is expected since arc injectors were designed to inject high  $\beta$  plasma in the cusp but not to sustain it.

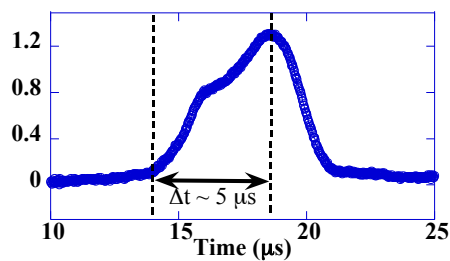
29

## Estimate of High $\beta$ Confinement Time

Theoretical model  
to estimate high  $\beta$  confinement time



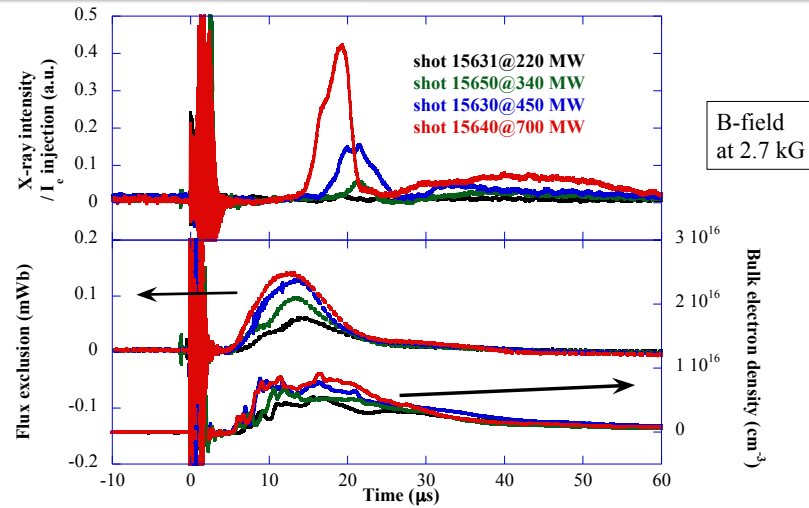
Experimental results  
Shot 15640



- Note the shape of x-ray intensity profile: a gradual rise and a rapid drop
- From time response of x-ray signal  $\rightarrow \tau > 2.5 \mu\text{s}$  ( $2 \times \tau \sim$  x-ray signal rise time)
- **2.5  $\mu\text{s}$  is about  $\sim 50$  times better than low  $\beta$  cusp confinement time**
- The observed confinement enhancement is very significant and compares well with the theoretically predicted high  $\beta$  cusp confinement time by Grad and his team

30

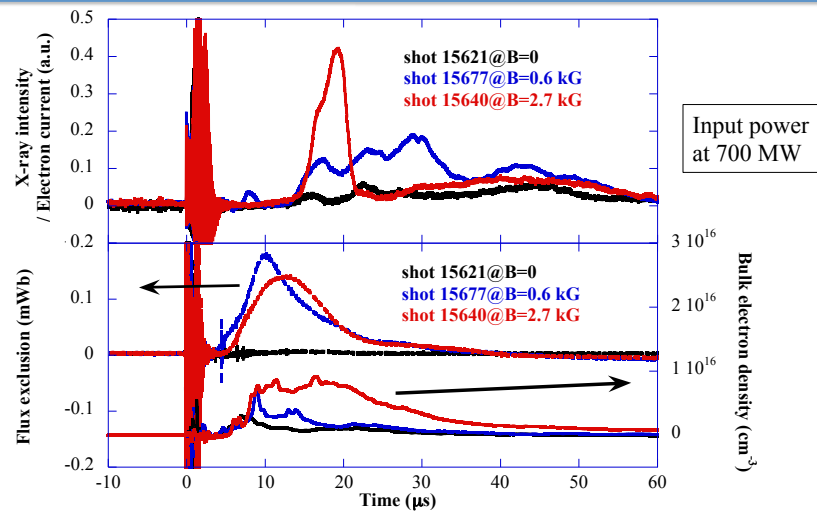
## Cusp confinement vs. Injection input power



Cusp confinement enhancement requires sufficiently high  $\beta$  plasma condition

31

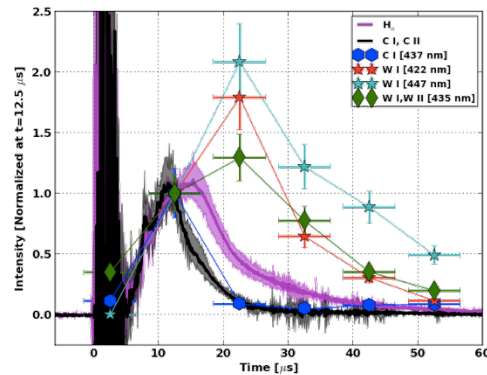
## Cusp confinement vs. initial B-fields



No confinement enhancement at B=0 but we need to do more to understand B-field effects

32

## Time resolved spectroscopy on W-impurity



Tungsten cathode  
after 200 shots

- Line emission intensities from main ion species (H and C) decay early
  - Despite plasma density decay (& cooling of plasma), Tungsten line intensities peak later in time and decay slowly --> indicates gradual build up of Tungsten impurity.
- > x-ray peak late in the shot (40-50 μs) is from e-bam interaction with Tungsten

33

## Our Findings on High $\beta$ Cusp Confinement

### Increase in X-ray signal

- Coincides with high  $\beta$  plasma state in the cusp
- Only observed when there is sufficient flux exclusion or plasma injection reaches a threshold
- Peak increase is 10-20x or more compared to low  $\beta$  state
- Exhibits asymmetrical time behavior: gradual increase followed by rapid decrease
- Clearly separated from W impurities injection in time domain

**We believe our x-ray measurements unambiguously validate the enhanced electron confinement in a high  $\beta$  cusp compared to a low  $\beta$  cusp**

34

## Unresolved issues on high $\beta$ cusp

### 1. Decay of good confinement phase

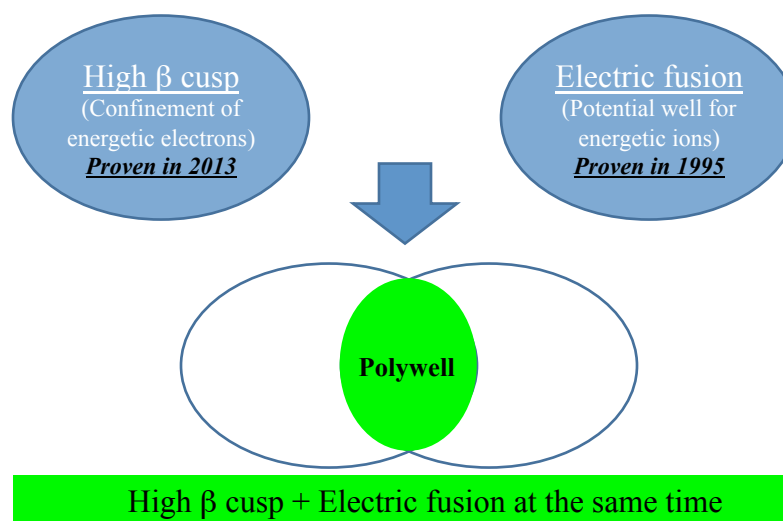
- Decay mechanism: plasma loss/plasma cooling or magnetic field diffusion or something else
- How to extend high  $\beta$  state and prevent the decay

### 2. Topological information on cusp magnetic fields during high $\beta$ state

- Thickness of transition layer
- Magnetic field lines near the cusp openings

35

## Future Work



36

## Summary

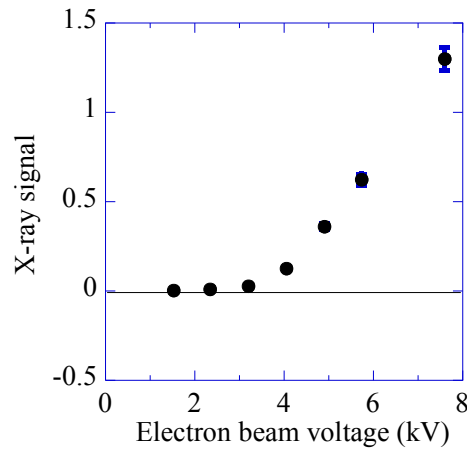
- Time resolved hard x-ray measurement provide the first ever direct and definitive confirmation of enhanced plasma confinement in high  $\beta$  cusp, a theoretical conjecture made by Grad and his team in 1950s.
- The enhanced electron confinement in high  $\beta$  cusp allows the Polywell fusion concept to move forward to complete the proof-of-principle test.
- If proven, Polywell device may become an attractive fusion reactor due to the following attributes
  - stable high pressure operation from cusp
  - good electron confinement by high  $\beta$  cusp
  - ion acceleration and confinement by electric fusion

37

## Supplemental Slides

38

## Confirmation of X-ray filter vs. beam energy

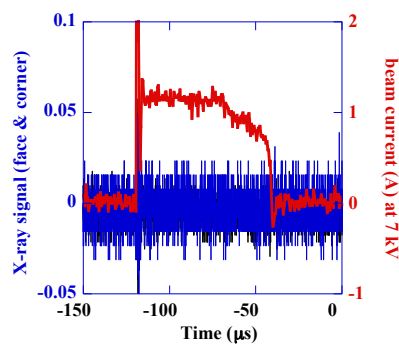


- X-ray was generated by electron beam on Stainless Steel target

- 25  $\mu\text{m}$  thick Kapton filter works well to eliminate X-ray photons below 2 keV

39

## Confirmation of X-ray collimation



- e-beam into vacuum magnetic field (no plasma) generates no x-ray response from the diode detector
- Indication of well collimated x-ray optics

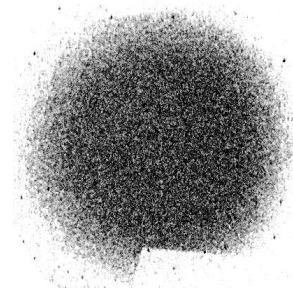


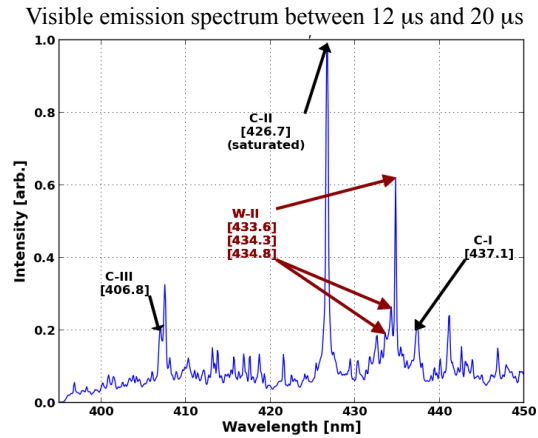
Image plate (x-ray film) exposure at the face cusp detector location

- Uniform exposure
- No sign of spatial structure from coils & walls
- 10 mTorr  $\text{N}_2$  gas target
- 20 ms exposure with 4A@7 kV e-beam
- B-field at 1.4 kG

40



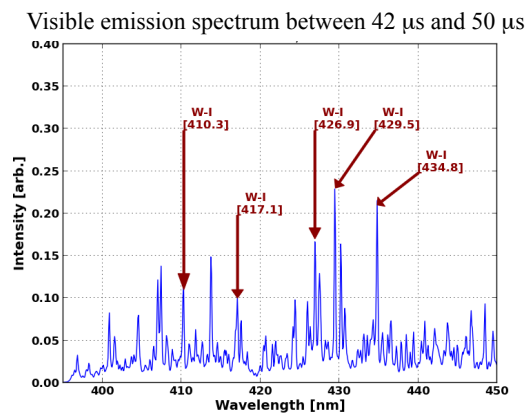
## Time resolved spectroscopy for impurity transport



**During the high  $\beta$  phase, plasma emission shows strong  $\text{C}^+$  lines & presence of  $\text{W}^+$  lines**  
 (Note that avg.  $n_e \sim 1.5 \times 10^{16} \text{ cm}^{-3}$  and  $T_e \sim 10 \text{ eV}$  during this period)

41

## Time resolved spectroscopy (cont.)



At later time, plasma emission is dominated by W neutral lines, while  $\text{C}^+$  and  $\text{W}^+$  lines disappear  
 (Note that avg.  $n_e \sim 0.2 \times 10^{16} \text{ cm}^{-3}$  and  $T_e < 10 \text{ eV}$ )

42